DESIGNING INTRAMEDULLAR POSTS FOR VETERINARY APPLICATIONS.

Estevam B. Las Casas[a], Leopoldo A. Paolucci[a], Rafael R Faleiros[b], Sergio S Rocha Junior[b], Paulo R. Fernandes[c], João Folgado[c], Luciano B. Rodrigues[d] and Luciana M. Gomides[e].

[a] Structural Engineering. Federal University of Minas Gerais
[b]Department of Clinical and Veterinary Surgery. Federal University of Minas Gerais
Av. Antônio Carlos , 6627. 31270-901 - Belo Horizonte – Minas Gerais – Brazil.
estevam.lascasas@gmail.com; leobia2009@yahoo.com.br; faleirosufmg@gmail.com
sergioveterinario@hotmail.com

[c]IDMEC, Instituto Superior Técnico, Universidade de Lisboa
Av. Rovisco Pais, 1049-001 Lisbon, Portugal
paulo.rui.fernandes@tecnico.ulisboa.pt; jfolgado@tecnico.ulisboa.pt

[d]State University of Bahia Southwest, Campus of Itapetinga, Itapetinga, Brazil
rodrigueslb@gmail.com

[e]Federal University of Itajubá, Campus of Itabira, Itabira, Brazil
lu_bh@hotmail.com

Keywords: Biomechanics, Interlocking Nail, Finite Elements, Bovine Femur.

Abstract: *The objective of this study is to describe the development of a low cost interlocking nail for young calves. Biomechanical parameters were measured for the numerical analysis of the bovine femoral repair system. Different polymeric and composite materials, polyacetal, polypropylene, polyamide and a glass fiber-reinforced polymer, were tested in silico to investigate their mechanical performance. Twelve femur models, divided into three groups, each one associated with a different fixation strategy, were used for simulation of an oblique simple fracture. Model loading conditions corresponded to a calf in transition (decubitus position to static position). The most critical stresses in the implant were found in the screws and at the interface between screw and nail. A numerical model demonstrated that all polymeric materials analyzed provided sufficient resistance to tolerate the loading imposed on the femur when an adequate fixation strategy was applied. After testing the biocompatibility of the material, in vivo tests will be conducted to validate the proposed design.*

1. Introduction

In cattle, fractures of long bones including femoral fractures are relatively frequent and great variety have been reported in the scientific literature [1- 4]. Diaphyseal femoral fractures in calves often occur following trauma during handling or a dystocia [2].
Several surgical techniques have been used in the stabilization of fractures of long bones: intramedullary pinning, cerclage wire, intramedullary interlocking nail fixation, rush pin fixation, bone plates and screws [1, 3]. The selection of treatment method depends on the

age of the animal, configuration of the fracture, and the surgeon's experience. Femoral fractures usually require some form of internal fixation [1].

Despite recent developments, long bone fractures in large animals, especially diaphyseal fractures, are still considered to be a challenge for veterinary surgeons, mainly due to animal size and mass. In many cases, euthanasia is still considered as a choice to avoid further financial loss and end suffering [4].

*Intramedullary interlocking nails (***IIN)** have been used in human surgery to repair fractures of the femur, humerus, and tibia. However, in veterinary orthopedics, the available products that are used in surgery to fix bone fragments are too expensive and are adapted from human devices [3]. Usually made with stainless steel, **IIN** may lead to stress shielding.

There is a clinical demand for developing implants specifically designed to be used in large animals. Several works have been developed by the biomechanics group of Federal University of Minas Gerais to develop polymeric **IIN** for application in veterinary orthopedics and to improve the surgical techniques applied in the repair of long bone fractures.

In calves the **IIN** is an interesting option, as the thin cortical layer of the humerus does not favor the application of orthopedic plaques, a usual treatment for these bones [5, 6].

In a previous work, the authors studied a system for internal immobilization of fractures in long bones with the use of *polypropylene (**PP**)***,** in the form of **IIN.** The reduction of fractures in the diaphysis of the humerus of newborn calves by **IIN** proved to be feasible, did not present complications in the postoperative period, allowed early use of the operated limb [6].

Another study evaluated, in vivo, *polyacetal (**POM**) and polyamide (**PA**)* nails in the form of **IIN** for immobilization of femoral fractures in young cattle. The nails did not resist the stresses when the animals returned from the postoperative period and failed [7].

The response of bovine bone in the presence of an implant was investigated using Finite Element Analysis (**FEA)** [8]; the remodelling results indicated that an **IIN** has the advantage over the metallic one of improving long-term bone healing and possibly avoiding the need of the implant removal.

FEA was used to model and estimate the performance of different polymers used in the construction of **IIN**: **POM**, **PP** and **PA** [9]. The results demonstrated that none of the polymers were sufficiently resistant to tolerate loading imposed on the femur during walking and that the screws closer to the fracture line are critical stress areas.

Recently, polymer composites have emerged as biomaterials that could potentially replace metallic alloys for use as orthopedic implants. Polyester resins in combinations with reinforcements such as glass fiber offer chemical resistance and excellent mechanical properties.

More recently three different polymers were used in the construction of **IIN**: **POM**, **PP, PA** and *glass fiber-reinforced polymer* (**GFRP)**. Fixation strategies were improved inspired in human orthopedic solutions, in an attempt to reduce stresses in critical regions observed in previous experiments [7, 9].

According to ongoing studies on the biocompatibility, **GFRP** may be apply in the manufacture of intramedullary nails for the treatment of fractures in calves (Rocha Junior, personal communication).

This work has two objectives: (i) use **FEA** to test the hypothesis that a polymeric nail (**GFRP**, **PP**, **PA** and **POM**) adapted for the characteristics of bovine anatomy may be able to stabilize a femoral fracture in calves and (ii) investigate the effect of different fixation strategies of the **IIN** on the mechanical behavior of a polymeric implant applied for femoral fracture fixation in calves.

2. Materials and methods

2.1. Sample

Five Holstein male animals with a mean weight (± SD) of 62.8 ± 20.4 kgf (range 41.0-85.0 kgf) and age 74 ± 15 days (range 60-90 days) were used in this study. All animals were evaluated by a veterinarian and considered clinically healthy, with no history of fractures. All procedures were evaluated and approved by the Ethical Commission on Use of Animals (CEUA) of UFMG, Brazil.

2.2. Data Collection

First the animals were conducted in a straight line so that they would step on the force plate (AMTI OR6-7 (©Advanced Mechanical Technology, Inc. USA)) with their right pelvic member. The animals were then placed lying down, with the right pelvic limb resting on the force plate and lifted while the measurement system acquired data on the ground reaction force. Three force measurements were taken for each animal. Contemplas (Contemplas, Germany) was used to synchronize force plate and video capture system (Basler pi A640, Germany) set to a frequency of 100 Hz.
The pelvic limb of the animals was modeled by four rigid bodies interconnected by the following joints: metatarsophalangeal, tibiotarsal, femorotibial and coxofemoral. These joints were represented by anatomical landmarks similar to those defined in [10]. The Simi-Motion 6.0 (Simi Reality Motion Systems, Germany) was used to digitize the acquired videos and measure the four bony segments, Fig. 1.

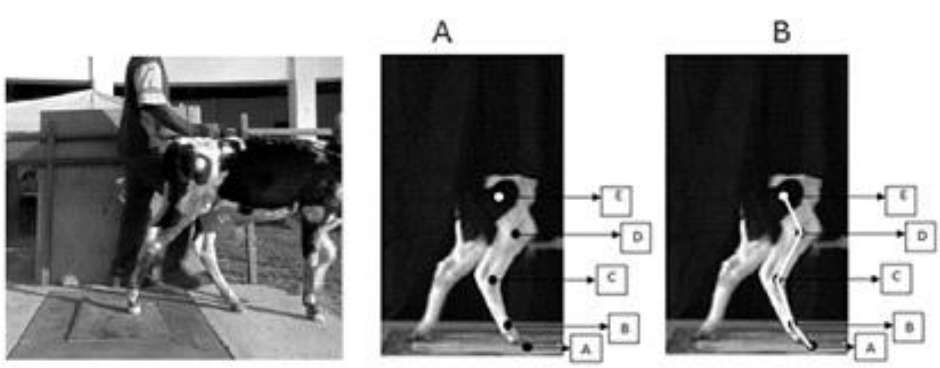

Figure 1: A) Bony landmarks (A) ground contact point; (B) point representing metatarsophalangeal joint; (C) point representing tibiotarsal joint; (D) point representing femorotibial joint (E) point representing coxofemural joint. B) Bone segments : AB (hoof); BC (metatarsus); CD (tibia) e DE (femur).
Source: Author’s database

2.3. Femoral Joint Load Determination

Coxofemoral joint loads were evaluated using static equilibrium and two-dimensional inverse dynamics. The routines for two-dimensional inverse dynamics were developed and implemented in MATLAB 2011. The input variables were body segment inertial properties **(BSIP)** values determined according to a parametric method described in [11]. The forces acting on the joints of the right pelvic limbs of the calves were determined when the ground reaction force (**GRF**) reached the peak in two conditions: during the walking gait, and during the transition from the decubitus position on the platform to the station position (**transition**). In the simulations, the forces during the **transition were considered** since their components presented higher values when compared with the values obtained during the walking gait. The muscle actions were not included as there was no information available about the muscular action in the joints of calves during the **transition.**

This research did not focus in the absolute values of stresses but in relative values. The results obtained as each of the three blocking conditions (**BLK**) was qualitatively compared to each other therefore the simplifications adopted in this research were quite acceptable.

2.4 Analysis of biocompatibility

The biocompatibility evaluation of GFRP, applied to build an IIN, was performed in vivo. A fragment measuring about 0.5 cm^2 was implanted in the subcutaneous of healthy rats after general anesthesia, Fig. 2. The implant remained in place for 45 days, where the intimate region of the implanted device was submitted to microscopic evaluation [12]. A commercial device similar to the test device was used as control.

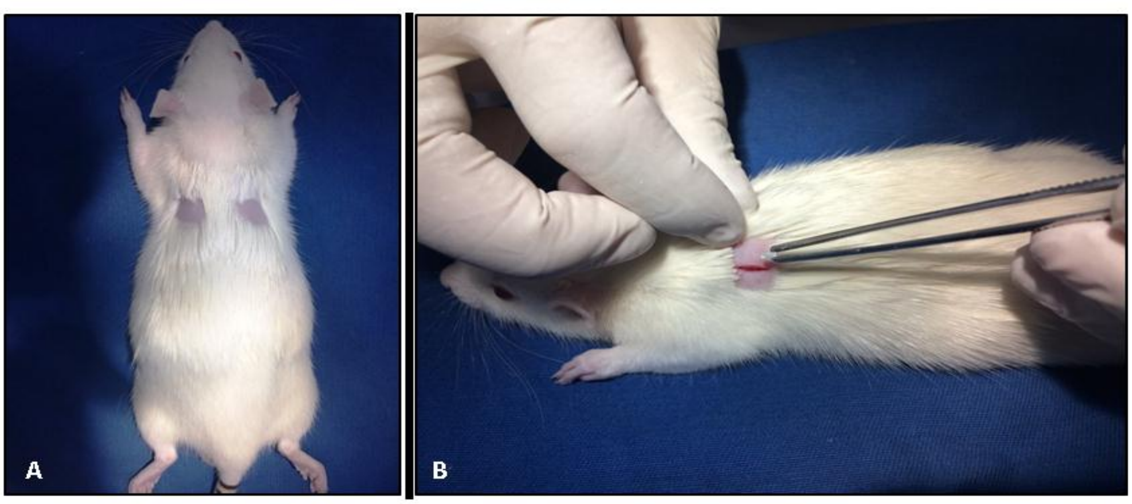

Figure 2: A) Tricotomy for insertion of fragments (right side - control), and GRPF (left side - experimental). B) Insertion of the fragment into the subcutaneous tissue of the animal.

Source: Author's database.

2.5. Finite Element Modeling

To construct a femur geometric model two animals and two cadaveric specimens underwent one CT session on axial tomography scanner Siemens, Somatom AR.T (Siemens, Germany). The animals were examined under general intravenous anaesthesia (xylazine (0.05 mg kg-1), ketamine (2mg kg-1) and midazolam (0.1mg kg-1).
The obtained DICOM (© NEMA Arlington Virginia) format images allows a three-dimensional reconstruction of the original anatomic structures, for this InVesalius 3.0 was used. This software allows separation of different tissues, bone and soft tissue (muscles and fat) by use of coloured masques (segmentation).
The masques were exported as a triangular mesh, in stl format, for refinement using Meshlab 1.3.3 (Instituto di Scienza e Tecnologie dell' Informazione, Italy). Then Meshlab meshes were exported to SolidWorks 2012 (Dassault Systèmes, , France).
A femur geometric model was obtained in SolidWorks and exported to Abaqus (Dassault Systèmes, France) and twelve finite element models were developed to simulate an oblique simple fracture (40°, grade A2 by the AO/ASIF score system).
The models were divided into three groups, with each group associated with a specific nail fixation strategy, referred as blocking condition (**BLK**) (Fig. 3).
Three **BLK** were used to block the **IIN.** The first **BLK** according previous study [8], two other blocking situations, suggested in a DePuy Synthes surgical technique manual, available for consultation at **http://osteosyntese.dk/wp-content/uploads/2014/11/**, noted as suitable for use in distal femur fractures human, were also studied.

Figure 3: A) 1st condition (**BLK1**) four lateromedial direction cortical screws. **B**) 2nd condition (**BLK2**) four lateromedial direction cortical screws, two at proximal diaphysis and two at distal condylar region. **C**) 3rd condition (**BLK3**) two lateromedial direction at distal condylar region and two caudocranial direction at proximal diaphysis.

The nails were blocked by four 4.5 mm stainless steel cortical screws, inserted perpendicular to the bone longitudinal axis. In **BLK1** the 1st screw was located 10 mm from the fracture line, and the 2nd was 10 mm from the 1st screw (Fig. 3 – A). In the **BLK2** and **BLK3** blocking conditions (Fig. 3 – B and Fig. 3 - C), at proximal diaphysis, the 1st screw was located 20 mm from the fracture line, and the 2nd was located 10 mm from the 1st screw. In the condylar region, the 1st screw was inserted below 10 mm of the epiphyseal line and the 2nd 10 mm from the 1st, adapted from [13].

The femoral head had its translation movements restricted. Only translations in the direction of an axis connecting the head to the center of the femorotibial joint were allowed. The most lateral point of the distal epicondyle had its translational movements, in the direction of the anteroposterior axis, restricted. The point considered as the center of the femorotibial joint had all its translational degrees of freedom restricted [14].

Contact interactions among the different materials were established by considering tie constraints, bone and nail bonded to the screws, as described in previous numerical studies [9]. No contact was considered between bone surface and nail, and contact between bones fragments was assumed to be frictionless.

Materials were modeled as homogeneous, isotropic and linear elastic. The mechanical constants used for the **GFRP** material were calculated from the Halpin-Tsai equations (Jones, 1999) and for **POM, PA** and **PP** were obtained from Black and Hastings (1998).

Mesh convergence analysis was performed until the error in maximum hip displacement and strain energy was reduced to 3% [14]. The load was applied as a concentrated force on the point of the femoral head in the direction of the axis formed by the center of the hip joint and a point chosen to represent the tibiofemoral joint and a moment in the proximal epicondyle region.

The maximum von Mises stresses were recorded for the screws and **IIN**, and the maximum principal stress was recorded for the bone. All values were compared to the yield and rupture points one of the four investigated materials, values above the yield point or rupture stresses were considered to be indicative of failure.

3. Results

3.1 Histopathological Diagnosis

After the histopathological tests performed according to ISO 10993-6: Biological evaluation of medical devices, Part 6: Tests for local effects after implantation (2007), the **GFRP** were considered as moderately reactive. The semi-quantitative evaluation (based on Hematoxylin and Eosin (**HE**) staining) presented score 5.0, thus becoming fit for use in vivo. Among the findings there was the formation of a neovascularization around the fragments, in addition, the formation of a fibrous capsule (Fig. 4).

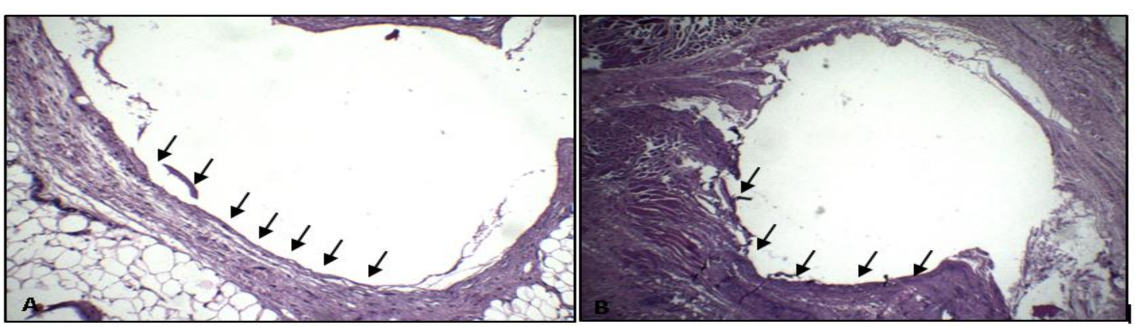

Figure 4: Photomicrography, HE staining, 4x magnification. Arrows indicate the formation of a fibrous capsule in the control group (4-A). Photomicrography experimental group findings similar to the control group (4-B).

3.1 Simulations

The screws and holes were numbered beginning at the most distal (1st screw) and proceeding to the most proximal (4th screw).

The **BLK1**, **BLK2**, and **BLK3** showed bone mean stress (± SD) of 89.53 ± 0.30 (range 89.30-90.04 MPa), 29.96 ± 0.04 (range 29.93-30.02 MPa), and 20.34 ± 0.22 (range 20.19-20.72 MPa) respectively.

The maximum principal stress values at the bone were always below yield and rupture points. The magnitude of stress with **BLK1** was higher than those presented with the other alternatives, regardless of the considered material (Fig. 5).

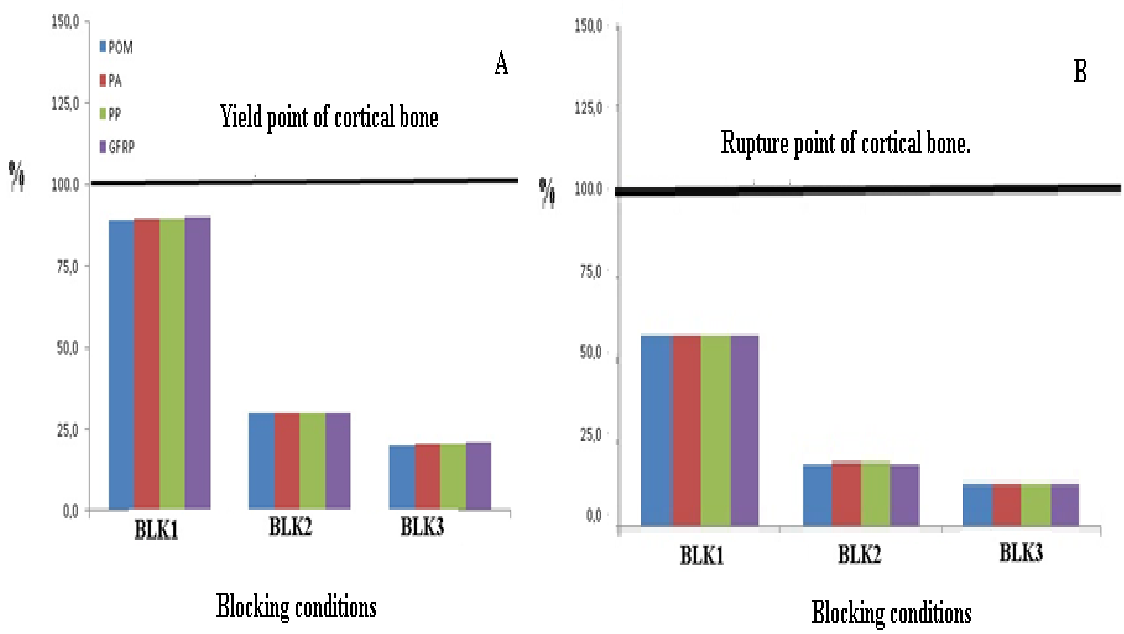

Figure 5: Percentages of maximum principal stresses in bones with different polymeric interlocking nails relative to the bone yield point (A) and relative to the bone compressive rupture point (B) when the bones were subjected to a load in a model of bovine femoral fracture.

The simulations showed that equivalent stresses on the nail in some cases exceeded the rupture point of the material. For **BLK1**, **POM**, **PA** and **PP** nails ruptured. Only the **GFRP** nail did not fail for **BLK1**. The **PP** nail also failed in the **BLK3**, and the equivalent stress values on the **PA** nail almost reached the yielding point of the material.

The values for the **GFRP** nail were not included in part B of the graph as the reference rupture value for the material was not found (Fig. 6).

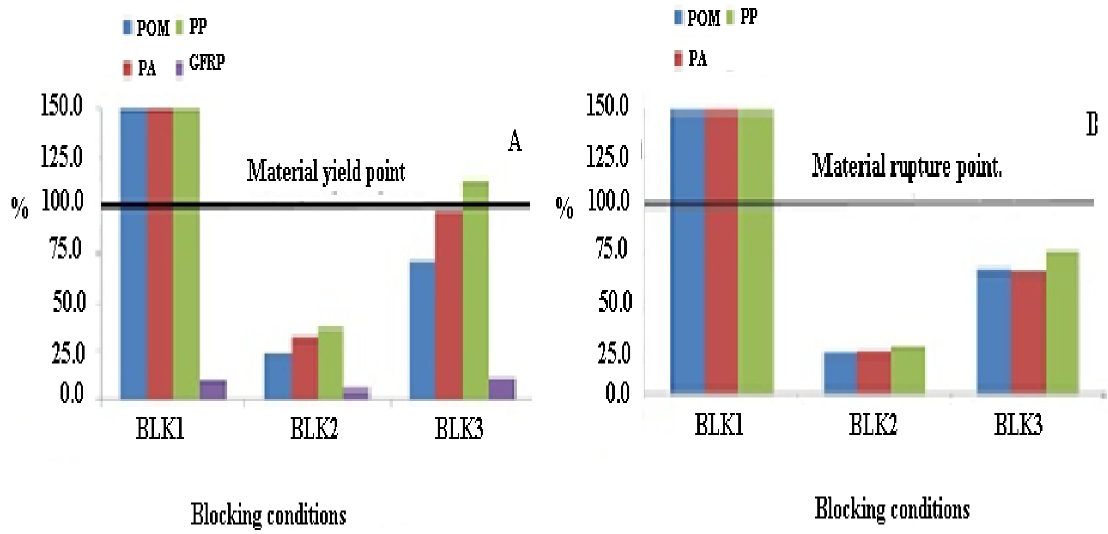

Figure 6: Percentage of maximum von Mises stress in different polymeric interlocking nails relative to the material yield point (A) and the compressive rupture point (B) when the bones were subjected to a load in a model of bovine femoral fracture.

For all materials, the maximum stress values at the bone model were found at the interface between the 1st screw and the screw hole for **BLK1** or **BLK2**. For **BLK3**, the maximum stress at the bone model occurred at the interface between the 4th screw and the screw hole. The maximum stress values at the nail for **BLK2** and **BLK3** were always found at the interface between the 1st screw and the screw hole. For **BLK1**, the stress values were dependent on the nail material. When **POM** and **PA** were used, the maximum values were found at the interface between the 1st screw and the screw hole. However, with the **PP** and **GFRP** nails, the maximum values occurred between the 3rd screw and the screw hole.

All values for the equivalent stresses in the screws were below the yield stress of stainless steel (205 MPa). The stresses in screws for BLK2 were always lower than stresses for BLK1 and BLK3 when the screws closer to the fracture line (2nd and 3rd) were analyzed (Tab. 1).

Material	Blocking condition	Stress (MPa)					
		Bone (hole)	Nail (hole)	Screw			
				1st	2nd	3rd	4th
POM	1st	89.30 (1)	154.20(1)	179.20	146.10	166.70	171.00
	2nd	29.93(1)	15.20(1)	29.98	18.43	22.24	107.4
	3rd	20.19(4)	46.28(1)	30.31	73.18	175.70	114.40
PA	1st	89.36(1)	130.20(1)	179.60	146.20	166.90	171.20
	2nd	29.97(1)	13.07(1)	26.69	15.85	22.27	103.10
	3rd	20.22(4)	38.88(1)	25.01	59.88	176.00	114.70
PP	1st	89.42(1)	103.70(3)	180.20	146.50	195.80	171.40
	2nd	30.02(1)	7.56(1)	21.56	14.86	22.32	103.40
	3rd	20.23(4)	22.80(1)	17.43	44.30	176.50	115.00
GFRP	1st	90.04(1)	90.75(3)	176.00	146.50	167.50	171.00
	2nd	29.92(1)	54.69(1)	23.93	18.87	21.94	101.30
	3rd	20.72(4)	102.80(1)	66.20	128.90	174.30	114.60

Table 1: Stress values for nails and screws (von Mises) and bone (maximum principal)

4. Discussion

In the simulations, the maximum stresses in the bone were found at the interface between screws and the screw holes, where the load transfer was the greatest. The current results showed that for the same **BLK**, the tensions in the bone model were quite similar for all polymeric materials. This finding is in agreement with the previous study [9] and suggests that bone tensions are dependent not only on the material used to build **IIN** but also on the strategy used to stabilize the fracture.

The simulations showed higher stresses at the interface between screw and hole nails. Interlocking screws placed proximal and distal to the fracture site restricted the translation and rotation at the fracture site, which is important in oblique fractures that rely on the screws for stability. However, the closer the distal screw was to the fracture, the less cortical contact the nail had, which led to increased stresses on the screws, putatively causes implant failure. This may explain why the polymeric nails failed in the presence of the bending forces generated in the **transition** [7].

Simulations with **BLK1** did not provide the necessary implant stability, and failures occurred in all polymeric nails except for the **GFRP** nail. Our results are in agreement with an *in vivo* study [6], in which all polymeric nails that were used in conditions similar to **BLK1** failed to fix femoral fractures in calves that were allowed to walk freely during the early postoperative period.

The use of the **BLK2** resulted in a reduction in the stress values on all screws. The stresses on the nails decreased approximately 58%, whereas the stress on the bone increased approximately 47% compared with the value for the **BLK3**.

This suggest that polymeric nails are less resistant to bending when **BLK3** is applied, thus increasing the contact area during loading, leading to an increase in the portion of loads carried by the bone. This finding agrees with previous studies that found increased loading levels on the bone when less stiff materials were used to manufacture intramedullary nails [15].

The **GFRP** nail was resistant to forces and moments applied to the femur model. The longitudinal glass fiber used to reinforce the composite nail may be responsible for increasing the nail rigidity, but this possibility cannot be confirmed without experimental validation.

In the simulations all of the materials used were resistant to deformation and rupture when the **BLK2** was used. When **BLK3** was used the **PP** nail failed, and the von Mises stress values on the **PA** nail almost reached the yield point of the material.

In the current study, the largest stress was found at the most distal nail hole. These simulations results are similar with a previous study with similar blocking conditions that found the largest equivalent von Mises stress at the same screw [15].

5 Conclusions

The early postoperative period is the most critical for the locking nail system since the load is entirely transferred through the nail and the blocking screws without any load sharing with the bone [16].

Several factors influence the performance of intramedullary nails in the fixation of fractures of long bones, such as the femur design, nail material, nail length, number and orientation of blocking screws, and distance from the blocking screws to fracture site [17].

The **FEA** indicates that all polymeric materials (**POM**, **PA**, **PP** and **GFRP**) provided sufficient resistance to tolerate the loading forces imposed on the femur during the transition when an adequate blocking strategy was applied.

6. Acknowledgment

The authors acknowledge the support of the Brazilian funding agencies FAPEMIG, CAPES and CNPq.

7. Disclosure Statement

The authors declare that they have no competing interests.

8. References

1. G. St-Jean, R.M. DeBowes, A.M. Rashmir, T.J. Engelken. Repair of a proximal diaphyseal femoral fracture in a calf, using intramedullary pinning, cerclage wiring, and external fixation. *Journal of the American Veterinary Medical Association*. 200,1701–1703, 1992.

2. J.G. Ferguson. Femoral fractures in the newborn calf: biomechanics and etiological considerations for practitioners. *Canadian Veterinary Journal*. 35,626–630, 1994.

3. H.P. Aithal, G.R. Singh, M. Hoque, S.K. Maiti, P. Kinjavdekar, Amarpal, A.M. Pawde, H.C. Setia. The Use of a Circular External Skeletal Fixation Device for the Management of Long Bone Osteotomies in Large Ruminants: An Experimental Study. *Journal of Veterinary Medicine A*. 51,284-293, 2004.

4. D.M. Nunamaker. On bone fracture and treatment in the horses. *Proceedings American Association of Equine Practitioners*. 48,90–101, 2002.

5. G.F. Hamilton, E.P. Tulleners. Transfixation pinning of proximal tibial fractures in calves. *Journal of the American Veterinary Medical Association*. 176(8),25-727, 1980.

6. C.A. De Marval. Ex-vivo and in vivo study of biocompatible polymer for manufacture of a blocked pin for humerus fracture reduction in calves. (in Portuguese). M. Sc. Thesis, Brazil, Universidade Federal de Minas Gerais, 2006.

7. O. Spadeto Junior, R.R. Faleiros, G.H.S. Alves, E.B. Las Casas, L.B. Rodrigues, B.Z. Loiacono, F. Cassou. Failure to use polyacetal and polyamide in the form of a blocked intramedullary nail (in Portuguese). *Ciência Rural*. 40(4), 907 – 912, 2010.

8. L.B. Rodrigues, D.S. Lopes, J. Folgado, P.R. Fernandes, E.B. Pires, E.B. Las Casas, R.R. Faleiros. Bone remodelling analysis of a bovine femur for a veterinary implant design. *Computer Methods Biomechanics and Biomedical Engineering*.12, 683–690, 2009.

9. L.B. Rodrigues, E.B. Las Casas, D.S. Lopes, J. Folgado, P.R. Fernandes, E.A.C.B. Pires, G.E.S. Alves, R.R. Faleiros. A Finite Element Model to Simulate Femoral Fractures in Calves: Testing Different Polymers for Intramedullary Interlocking Nails. *Veterinary Surgery*. 41(7), 838-844, 2012.

10. A.H. Herlin, S. Drevemo. Investigating locomotion of dairy cows by use of high speed cinematography. *Equine Veterinary Journal*. 29, 106–109, 1997.

11. L.A. Paolucci, L.M. Gomides, E.B. Las Casas, R.R. Faleiros , A.G.P. Andrade, **C.** Paz, V. Fedotova, **H.** Menzel. Estimation of bovine pelvic limb inertial properties using an elliptical model. *Journal of the Brazilian Society of Mechanical Sciences and Engineering*. 9, 2371–2382, 2017.

12. ISO 10993-6: Biological evaluation of medical devices. Part 6: Tests for local effects after implantation, 2007.

13. DePuy Synthes. Expert R/AFN Retrograde/Antegrade Femoral Nail, Surgical Technique. 2016.

14. R. Bayoglu, F. Okyar. Implementation of boundary conditions in modeling the femur is critical for the evaluation of distal intramedullary nailing. *Medical Engineering & Physics.* 37, 1053-1060, 2015.

15. G. Cheung, P. Zalzal, M. Bhandari, J.K. Spelt, M. Papini. Finite element analysis of a femoral retrograde intramedullary nail subject to gait loading. *Medical Engineering & Physics.* 26, 93–108, 2004.

16. R. Montanini, V. Filardi. In vitro biomechanical evaluation of antegrade femoral nailing at early and late postoperative stages. *Medical Engineering & Physics*.32, 889–897, 2010.

17. A.J. Thakur. Elements of Fracture Fixation. 2ª ed. Elsevier Health Sciences. 2012.